THE ASTROPHYSICAL JOURNAL, 456:833–839, 1996 January 10

INTERPRETATION OF THE OBSERVED PLASMA "TURBULENT" VELOCITIES AS A RESULT OF MAGNETIC RECONNECTION IN SOLAR FLARES

ESTER ANTONUCCI AND CARLO BENNA
Istituto di Fisica Generale, University of Torino, Torino, Italy

AND

BORIS V. SOMOV
Sternberg State Astronomical Institute, Moscow State University, Moscow, Russia
Received 1995 May 8; accepted 1995 July 20

ABSTRACT

One of the distinctive features of magnetic reconnection in current sheets, which has been proposed as the primary energy source in solar flares, is the presence of fast plasma outflows, or jets, whose velocities are nearly equal to the Alfvén speed and depend mainly on the electron and ion temperatures inside the current sheet. We briefly discuss the outflows that originate during the reconnection process in the high-temperature turbulent current sheet (HTTCS) approximation, both for preflare and "hot" phase conditions. Outflows can give rise to plasma velocity distributions with equal and opposite components along the line of sight, and therefore they can, in this way, create a symmetric, nonthermal broadening in the soft X-ray lines observed during solar flares. A comparison of the nonthermal profiles of the Fe XXV emission lines observed at flare onset with the predictions of the HTTCS model suggests that the observed nonthermal broadenings are consistent with the presence in the flare region of several small-scale or one (or a few) curved, large-scale reconnecting current sheets with internal temperature $\leq 8 \times 10^7$ K. The velocities of the outflows at the emergence of the reconnecting current sheets are inferred to be ≤ 1100 km s^{-1}.

Subject headings: MHD — Sun: flares — turbulence

1. INTRODUCTION

According to our present views, the accumulation of the "free magnetic energy" necessary to energize solar flares and its rapid conversion into different forms of kinetic energy, namely, the energy of fast hydrodynamic flows, or jets, the thermal energy of high-temperature plasma, and the kinetic energy of accelerated particles, occur in reconnecting current sheets present in active regions (see, e.g., Syrovatskii 1976; Priest 1982; Zirin 1987; Tandberg-Hanssen & Emslie 1988; Antonucci & Somov 1992). To obtain direct observations of reconnecting current sheets is not a simple task, as their emission measure is very small in comparison with the emission measure of the high-temperature plasma produced by the flare energy release through the chromospheric "evaporation" process, that is, through the convection of heated chromospheric plasma into the corona (Antonucci et al. 1982; Antonucci, Gabriel, & Dennis 1984). The current-sheet emission measure is also small in comparison with that of the plasma heated inside the current sheet, which is ejected through its edges and accumulates in the ambient solar atmosphere.

Therefore, very specific properties of reconnecting current sheets should be used in an attempt to infer their presence in the solar corona. The most outstanding of these properties have been indicated by Parker (1957) and Sweet (1958), who have shown that plasma is expelled from a stationary reconnecting current sheet in two opposite directions with a velocity comparable to the Alfvén speed. This means that, in the upper chromosphere and lower corona, the velocities of such jets may be as high as 1000 km s^{-1} (see, e.g., Syrovatskii & Somov 1980). These plasma outflows produce a symmetrical broadening of the optically thin spectral lines that is significantly larger than the thermal one, as we shall show in this paper.

Reconnecting current sheets appear as a result of photospheric plasma motions, which displace the footpoints of the magnetic field lines. Photospheric motions consist of two different components: a regular and a chaotic one. Regular motions in the photosphere are well known; they include emergence of a new magnetic flux, large-scale horizontal vortex flows, and shear flows. All induce a regular, large-scale evolution of the magnetic field in the corona. As a result of this regular evolution of coronal fields, large-scale current sheets appear where magnetic fluxes of opposite polarity interact and change their "connectivity," i.e., they reconnect. As an example, we can consider a reconnecting current sheet, forming between a new emerging flux and the magnetic field that preexists in the corona, as the magnetic field of an active region as a whole. In the opposite limiting case, we find small-scale chaotic flows that are created in the photosphere by turbulent motions. In this case, thin magnetic tubes interact and reconnect in many sites in the corona (Parker 1979).

In principle, the nonthermal broadening of spectral lines in solar flares can also be explained by invoking, for example, MHD turbulence, which is isotropic under the assumption of a weak magnetic field—that is, when the magnetic energy density is small in comparison with the thermal energy of the plasma and the kinetic energy of its turbulent hydromagnetic motions. This case occurs in the photosphere outside sunspots. On the other hand, for strong magnetic fields one can expect in the upper chromosphere and low corona a one-dimensional distribution of velocities along the field lines. This distribution can be symmetric if the magnetic field is uniform over the typical linear scale of turbulence. If such turbulence is indeed responsible for the solar-flare mechanism, then the observed nonthermal broadening of the XUV lines can be interpreted to

be a manifestation of "real turbulent velocities." However, up to now we do not have any serious observational evidence for this model of solar flares.

Hydrodynamic vortex flows of high-temperature plasma in the corona can have a symmetric velocity distribution along the line of sight. However, there is no observational evidence for such flows in flare plasmas. From the theoretical point of view, it is difficult to imagine the existence of many vortexes in a strong magnetic field since they would have to produce a great deal of magnetic energy under the frozen-in condition in the coronal plasma. To the same extent, pinch flows near electric current or many current filaments can, in principle, yield the same observational effect of nonthermal broadening in the XUV lines although a problem may arise with pinching of high-temperature plasma if this plasma already has high pressure. In any event, difficulties do arise with a model that assumes pinching in one or many points when we try to explain other observational features of solar flares as a general phenomenon as well as individual events. This is because a solar-flare model has to explain, at least, the energy-release power and the three-dimensional structure of a flare, which has to be consistent with its images in XUV and other wavelength bands. Furthermore, a flare model should also explain the observed dynamics as well as the acceleration of particles (see Somov 1994).

2. MODEL FOR RECONNECTING CURRENT SHEETS AND INTERPRETATION OF NONTHERMAL LINE PROFILES IN SOLAR FLARES

We suggest, after Antonucci, Rosner, & Tsinganos (1986), that the nonthermal line broadening and the associated nonthermal or "turbulent" velocity observed at flare onset may be related to the existence of one or several (maybe, many) current sheets where magnetic field lines are reconnecting. In general, in flare conditions, we expect the existence of one, or a few, large-scale reconnecting current sheets or, alternatively, many small-scale sheets (the latter have also been suggested to be responsible for the "steady" heating of an active region). In any case, current sheets cannot be observed in a direct way, but we propose that they can be detected indirectly through the plasma ejected during reconnection.

The velocity distribution of the high-temperature plasma near each reconnecting current sheet can be described by consideration of a simple configuration of magnetic fields, such as in Figure 1. In the figure, v_d is the drift velocity, or reconnection velocity, induced by the change of configuration of the coronal magnetic fields in response to the plasma motion in the photosphere; V_A is the Alfvén velocity, which is the velocity of plasma outflows, or jets, from the current sheet. We can apply the high-temperature turbulent current sheet (HTTCS) model (see Somov 1992, pp. 115–219) when the following conditions, which are verified in the solar corona during flares, are satisfied:

1. The Alfvén velocity is much larger than the drift velocity: $V_A \gg v_d$, which implies that the approximation of a strong magnetic field (Somov & Syrovatskii 1976) is valid in the coronal plasma near the current sheet;
2. The temperature of plasma inside the HTTCS is much higher than the temperature of the ambient plasma; for this reason, the anomalous thermal fluxes are important in the energy balance of the HTTCS and, hence, in the energy output of solar flares.

In what follows, we explore whether the nonthermal broadenings of the soft X-ray lines emitted during solar flares can be related to the velocity distribution of the high-temperature plasma expelled during reconnection from a current sheet, using the HTTCS model.

The average outflow velocity along the line of sight (LOS) of the observer is related to the Alfvén velocity as follows:

$$V = V_A \cos \alpha , \tag{1}$$

where α is the angle between the LOS and the direction of plasma outflows (Fig. 1). Here the Alfvén velocity for the plasma outflows is

$$V_A = B_0(4\pi M n_s)^{-1/2} , \tag{2}$$

where B_0 is the reconnecting component of the magnetic field near the HTTCS, n_s is the plasma density inside the HTTCS, and M is the average "molecular" weight (for plasma with solar abundance of elements $M \approx 1.44 m_p$, where m_p is the proton mass).

Let us suppose that stationary reconnection occurs; that is, there is a balance of magnetic and gas pressure across the HTTCS:

$$\frac{B_0^2}{8\pi} = n_s k(T_{e,s} + T_{i,s}) , \tag{3}$$

where $T_{e,s}$ and $T_{i,s}$ are the electron and ion temperatures of the plasma inside the current sheet, respectively. This expression allows us to rewrite equation (2) as follows:

$$V_A(T_s) = \sqrt{\frac{2k}{M}}(1 + \theta^{-1})^{1/2}\sqrt{T_s} , \tag{4}$$

where θ is the electron-to-ion temperature ratio, $T_s = T_{e,s}$, and $T_{i,s} = \theta^{-1} T_s$.

We thus rewrite equation (1) for nonthermal or "turbulent" velocity as

$$V(T_s) = \sqrt{\frac{2k}{M}} f(\theta)\sqrt{T_s} \cos \alpha , \tag{5}$$

where

$$f(\theta) = (1 + \theta^{-1})^{1/2} . \tag{6}$$

Considering the symmetry of the current sheet of Figure 1, one can see that the average outflow velocities are projected into two opposite components $V(T_s)$ along the LOS, one at each edge of the current sheet. The result is a symmetric broadening of the XUV lines emitted by the plasma ejected out of the current sheet.

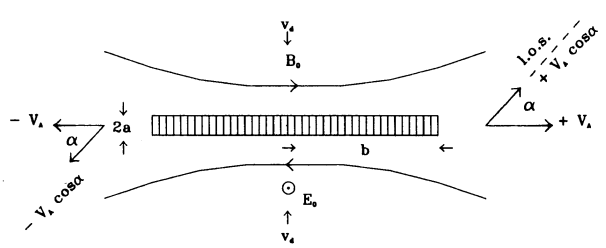

FIG. 1.—Magnetic field lines and high-temperature plasma velocities near a reconnecting current sheet.

2.1. *Main Phase of Flare Evolution*

The value of the ratio θ depends on the state of plasma turbulence in the HTTCS. For example, for a nonneutral HTTCS, that is, one with a small transverse component B_t of the magnetic field, in the marginal regime of ion-acoustic turbulence we obtain $\theta = 6.5$, so that $f(\theta) = 1.1$; then,

$$V(T_s) = V_A(T_s) \cos \alpha \approx 1.2 \times 10^4 \sqrt{T_s} \cos \alpha \text{ cm s}^{-1} , \quad (7)$$

where the temperature is measured in kelvins. These conditions apply to the case of the "hot" phase of solar-flare evolution (Somov 1992). The value of $V(T_s)$ does not depend on the value of the transverse field B_t. $V(T_s)$ represents an upper limit of the nonthermal or "turbulent" velocity because it is the value of the outflow velocity at the emergence from the HTTCS, before the outflows undergo possible deceleration processes in the ambient plasma surrounding the current sheet.

In order to account for projection effects along the LOS, let us consider the two possible extreme cases. In the case of a single, large-scale current sheet with no preferential orientation, we expect, by averaging over a large number of reconnection events, an average projection angle:

$$\langle \cos \alpha \rangle = \tfrac{1}{2} . \quad (8)$$

If reconnection occurs in many small-scale regions instead of a large-scale current sheet, we obtain, in the assumption of a uniform distribution of projection angles of the current sheets, the same mean square value $\langle \cos \alpha \rangle = \frac{1}{2}$ for an individual flare; i.e., in the first case, the averaging is performed over a large number of flares, in the second case over a large number of reconnection regions existing in the volume where a single flare occurs.

A real large-scale current sheet, though, is in general not contained in a plane as in Figure 1 but consists of a curved surface. In this case, the angle of the outflow velocity α changes along the lines that define the edges of the current sheet. The mean square value of the projection angle is therefore dependent on the real shape of the current sheet, and it may tend to $\langle \cos \alpha \rangle \sim \frac{1}{2}$ when the increasing complexity of the current-sheet configuration leads to an almost uniform distribution of α angles. A curved current sheet may also have the effect of introducing, in addition to the symmetric broadening, a nonsymmetrical effect in spectral lines when the velocity distributions at the edges of the current sheet are not symmetric.

According to Somov (1992), reasonable values of T_s in the HTTCS for the "hot" phase of flare evolution are

$$T_s \approx (70\text{–}160) \times 10^6 \text{ K} ;$$

by using equations (7) and (8), we obtain for the expected nonthermal velocities

$$V \approx 500\text{–}760 \text{ km s}^{-1} .$$

It is interesting to compare the values obtained for turbulent velocities with the thermal velocity of calcium and iron ions, the spectra of which are more commonly studied in solar flares:

$$V_{\text{th},i}(T_s) = \sqrt{\frac{2k}{M_i}} \sqrt{T_s} , \quad (9)$$

where $M_i = A_i m_p$, A_i the element's atomic mass number.

The observed outflow velocity can be related to the thermal velocity of the ions within the current sheet by the formula

$$V(T_s) = V_{\text{th},i} 0.8 f(\theta) \sqrt{A_i} \cos \alpha ; \quad (10)$$

in particular, for Ca ions we have $M_i = 40.1 m_p$ and

$$V_{\text{th,Ca}}(T_s) = 2 \times 10^3 \sqrt{T_s} . \quad (11)$$

Therefore, in the temperature range $T_s = (70\text{–}160) \times 10^6$ K, the thermal velocity of Ca ions is

$$V_{\text{th,Ca}} \approx 170\text{–}250 \text{ km s}^{-1} .$$

In the same temperature range for the Fe ions, for which $M_i = 55.8 m_p$, the velocities are

$$V_{\text{th,Fe}}(T_s) = 1.7 \times 10^3 \sqrt{T_s} , \quad (12)$$

$$V_{\text{th,Fe}} \approx 140\text{–}215 \text{ km s}^{-1} .$$

By comparing V with $V_{\text{th,Ca}}$ and $V_{\text{th,Fe}}$ we conclude that the expected "turbulent" velocities of Ca and Fe ions generated by the expulsion of plasma from a reconnecting current sheet are of the same order of magnitude but larger than their thermal velocities. Hence, we expect a nonthermal broadening observed in soft X-ray line profiles to be ascribed in part to the thermal motions of ions and in part to outflows.

2.2. *Preflare Phase of Flare Evolution*

In the preflare state, with reasonable physical parameters assumed for the region of magnetic reconnection, the marginal regime of ion-cyclotron instability seems to be more realistic than the ion-acoustic one (Somov 1992). In this case, $\theta = 0.33$; therefore, $f(\theta) = 2.01$ and

$$V(T_s) \approx 2.2 \times 10^4 \sqrt{T_s} \cos \alpha \text{ cm s}^{-1} . \quad (13)$$

For a preflare temperature $T_s \approx 4 \times 10^6$ K of the HTTCS, $V \approx 440 \cos \alpha$ km s^{-1}. In this approximation, from equations (8) and (13) we arrive at the conclusion that in the preflare reconnecting current sheet we should expect nonthermal velocities of the order of $V \approx 220$ km s^{-1}.

2.3. *Explosive Phase of Flare Evolution*

Let us also briefly discuss the more general case in which the equilibrium balance (eq. [3]) has not yet been reached in the magnetic-reconnection region. This may be, for example, the case of nonsteady reconnection during the transition from the regime of ion-cyclotron turbulence in the preflare precursor phase to the ion-acoustic turbulence at the onset of the impulsive phase of solar flares.

For this particular situation we have to add some unknown term X on the right-hand side of equation (3):

$$\frac{B_0^2}{8\pi} = n_s k T_s (1 + \theta^{-1}) + X . \quad (14)$$

The additional term X plays the role of an additional energy density, such as the kinetic energy of plasma motion inside a reconnecting current sheet, plus a quantity that depends on the time derivatives. The last term may be the most important during the stage of fast evolution of a reconnecting current sheet, corresponding to its rupture. In any event, the term X cannot be negative. Hence, instead of equation (5), we can use

$$V(T_s) = \sqrt{\frac{2k}{M}} \sqrt{T_s (1 + \theta^{-1}) + Y} \cos \alpha , \quad (15)$$

where the additional term

$$Y = \frac{1}{n_s k} X \quad (16)$$

provides a positive contribution to the turbulent velocity, in comparison with equation (5). It means that the observed turb-

ulent velocity may be larger than that predicted by equation (5) if, for example, nonsteady processes are essential, as at the onset of the impulsive phase of solar flares.

3. OBSERVATIONS OF NONTHERMAL VELOCITIES IN THE "HOT" PHASE OF SOLAR FLARES

Nonthermal line broadenings in flares have been observed by analysis of the profiles of lines emitted in the soft X-ray domain obtained with the high-resolution soft X-ray spectrometers flown during the maximum of cycle 21 (with, e.g., the bent crystal spectrometer [BCS] of the *Solar Maximum Mission* [*SMM*]). In this section, we compare the nonthermal line broadenings predicted on the basis of the velocity distributions of the plasma flowing out of a reconnecting current sheet in the HTTCS approximation with observation. As discussed in § 2, outflows should give origin to a symmetric, nonthermal broadening in the soft X-ray lines because of the fact that the average outflow velocities are in general projected in two opposite components of the same magnitude along the observer's LOS (see Fig. 1).

The phenomenology of nonthermal broadenings in solar flares has been studied in detail, mainly in analyses of the Ca XIX emission, the results of which have been reviewed by many authors (e.g., Doschek et al. 1986; Antonucci 1986, 1989; Doschek 1989). According to the results of these studies, the nonthermal excess in line width is larger at flare onset, when the difference between the Doppler temperature T_D, derived from the total observed line width, and the electron temperature T_e, derived from line ratios, is consistent with nonthermal velocities up to ~ 200 km s^{-1}. Toward the maximum soft X-ray emission, the nonthermal broadening decreases considerably, and in the decay phase the line width is either consistent with nonthermal velocities ≤ 60 km s^{-1} or nearly thermal ($T_D \sim T_e$).

The onset of nonthermal motion as observed in Ca XIX in general precedes that of the convective motion caused by chromospheric evaporation, which is signaled by the appearance of a blue component in the spectral emission (Antonucci et al. 1984). According to the results of Antonucci & Dodero (1995), who analyzed the lines observed with the flat crystal spectrometer (FCS) on *SMM* in the temperature range from 3 to 50×10^6 K, nonthermal velocities in the flare plasma increase with plasma temperature according to the same law that can be used to express the temperature dependence of nonthermal motions throughout the different temperature regimes of the solar atmosphere, from 10^4 to 10^7 K.

3.1. *Method of Analysis*

In the present analysis, we mainly study the nonthermal broadenings of the Fe XXV lines formed at temperatures close to the high temperatures expected in reconnecting current sheets during solar flares. The analysis includes both the Fe XXV and Ca XIX spectra emitted in a set of 20 flares, of classes M and X, observed with the BCS during 1980 (Table 1). The Fe XXV emission in a flare is in general observed with some delay with respect to the Ca XIX emission, presumably because of the higher temperature of formation of Fe XXV (the contribution functions of Ca XIX and Fe XXV peak at 30×10^6 K and 50×10^6 K, respectively). The first significant Fe XXV emission is detected with the BCS within an interval of 2 minutes (60 s on the average) before the peak of the hard X-ray burst (as measured in the energy range from 25 to 386 keV with the hard X-ray burst spectrometer on *SMM*) except in two cases, the 1980 November 6 and November 19 events, which are characterized by an initial, long-duration plateau in hard X-ray emission preceding the major burst.

TABLE 1

FLARES INCLUDED IN THE ANALYSIS

Date (1980)	Time (UT)	Active Region	Class	Coordinates
8 Apr	0304	2372	1B, M4	N12, W13
10 Apr	0917	2372	1N, M4	N12, W42
13 Apr	0403	2372	1F, M1	N10, W77
30 Apr	2020	2396	SN, M2	S13, W90
9 May	0712	2418	1B, M7	S21, W32
21 May.....	2055	2456	2B, X1	S14, W15
25 Jun	1550	2522	1B, M4	S29, W28
29 Jun	0233	2522	–, M3	S29, W90
29 Jun	1041	2522	–, M4	S29, W90
29 Jun	1822	2522	–, M4	S29, W90
1 Jul	1626	2544	1B, X2	S12, W38
21 Jul.....	0254	2562	1B, M8	S14, W60
23 Aug	2127	2629	1B, M2	N16, W39
24 Aug	1608	2629	SB, M1	N17, W52
25 Aug	1256	2629	SB, M1	N18, W62
24 Sep.....	0732	2684	1B, M1	N18, W25
5 Nov	2226	2776	1B, M1	N11, E07
5 Nov	2233	2776	1B, M4	N11, E07
6 Nov	1725	2779	2B, M4	S09, E65
19 Nov	0532	2779	–, M6	S10, W90

The presence of a nonthermal excess in line width is determined by analysis of the profiles of the Fe XXV resonance lines with a fitting technique. The observed Fe XXV spectrum is fitted with a synthetic spectrum in the interval from 1.840 to 1.890 Å by adjustment of the electron temperature, Doppler temperature, and ratio of the populations of adjacent ion stages, as described in Antonucci, Dodero, & Martin (1990). The plasma electron temperature T_e is determined with high precision by a best fit to the dielectronic satellites and the resonance line. The derived value is an average over the plasma temperature distribution in the flare region weighted with the contribution functions of the temperature-dependent lines considered in the fit. The accuracy of the temperature measurement depends mainly on the uncertainty in the atomic-physics parameters. The Doppler temperature T_D is derived from the total width of the line, previously corrected for the Lorentzian broadening due to the instrumental response. T_D is related to the half-width of the Gaussian fit of the line profile by the formula

$$g = \frac{\lambda}{c}\sqrt{\frac{2kT_D}{m_p A_{Fe}}}, \tag{17}$$

where A_{Fe} is the iron atomic mass number.

The observed nonthermal or "turbulent" velocity is proportional to the nonthermal excess in line broadening, which is a function of the difference between T_D and T_e:

$$V_{nt} = \sqrt{\frac{2k(T_D - T_e)}{m_p A_{Fe}}}. \tag{18}$$

When line profiles are affected by the presence of blueshifts, which are related to the occurrence of chromospheric evaporation, they are analyzed by use of a two-component fit (Antonucci et al. 1982). The determination of the parameter T_D, which measures the line broadening, is not influenced by the presence of an excess blue emission since it can be measured by fitting the red side of the resonance line profile. The different methods to detect the presence of blueshifted components in

the soft X-ray profiles of the impulsive phase of flares have been recently discussed by Mariska (1994) and Doschek et al. (1994).

3.2. *General Properties of Nonthermal Velocities Derived from* Fe XXV *Spectra*

The analysis of the Fe XXV spectral emission observed during flares allows us to derive three main properties of nonthermal velocities. First, the peak of nonthermal velocities is found just prior to or at the peak of the hard X-ray burst, which presumably corresponds to the time of maximum energy release in solar flares. Second, nonthermal velocities are mostly independent of flare longitude. Third, nonthermal velocities in the plasma that is emitting Fe XXV are significantly larger than those derived from the relatively cooler plasma that emits the Ca XIX lines.

In all flares, the first significant Fe XXV spectrum shows a nonthermal width much enhanced with respect to that of the lines emitted at the end of the rise phase and during the decay, when lines sometimes are thermal within the statistical errors ($V_{nt} \sim 0$). The highest value of nonthermal velocity $V_{nt,max}$ in a flare is in general found in the first or second significant Fe XXV spectrum, that is, either within ≤ 1.5 minutes before or in correspondence with the peak of the hard X-ray burst. The average delay between the peak in V_{nt} and the peak in hard X-ray emission is ~ 30 s. In approximately 50% of the disk flares included in the set of events analyzed, the peak of nonthermal velocity was reached before the onset of chromospheric evaporation. In the remaining 50%, the average delay of the peak relative to the onset of evaporation is on the order of 30 s.

Nonthermal velocities on the average are of the same order in limb and disk flares. For Fe XXV emission, the average nonthermal velocity $\bar{V}_{nt,max}$ is 170 ± 40 km s^{-1} for limb events and 180 ± 20 km s^{-1} for disk flares. This is consistent with the results obtained from the analysis of the Ca XIX spectra, $\bar{V}_{nt,max} = 100 \pm 40$ km s^{-1} for disk flares and 120 ± 30 km s^{-1} for limb flares (Antonucci et al. 1984). Therefore, the comparison between disk and limb events confirms that nonthermal velocities are independent of longitude, within the statistical errors. Furthermore, the substantial agreement between the disk and limb results shows that the contribution of blueshifts, related to chromospheric evaporation, to line profiles has been correctly taken into account in the analysis.

If we average over all flares independently of longitude, we find a nonthermal velocity of 180 ± 30 km s^{-1} for Fe XXV and 110 ± 20 km s^{-1} for Ca XIX. That is, nonthermal velocities increase significantly with the temperature of the emitting plasma, which has an average temperature for the Fe XXV and Ca XIX sources within $(13–25) \times 10^6$ K and $(11–20) \times 10^6$ K, respectively. The peak of the nonthermal velocity $V_{nt,max}$ obtained in individual flares from the analysis of the Fe XXV line profile is also dependent on temperature (Table 2). This is clearly shown in Figure 2, where limb and disk events are indicated with different symbols. In the range of temperatures between 13 and 25×10^6 K, nonthermal velocities range between 130 and 230 km s^{-1}. These are not the highest temperatures measured from the Fe XXV emission during flares since the maximum temperature $T_{e,max}$ is reached at the end of the rise phase, which occurs well after the peak of nonthermal velocity, reached in general near flare onset. When the plasma temperature reaches its maximum value, within $(17–26) \times 10^6$ K, nonthermal velocities decrease to values between 50 and 170 km s^{-1}.

TABLE 2

NONTHERMAL VELOCITIES IN FLARE PLASMAS

		Fe XXV		Ca XIX	
DATE (1980)	TIME (UT)	$V_{nt,max}$ (km s^{-1})	T_e (10^6 K)	$V_{nt,max}$ (km s^{-1})	T_e (10^6 K)
8 Apr	0304	214	15.0	164	14.5
10 Apr	0917	158	16.0	124	12.7
13 Apr	0403	192	16.0	148	12.0
30 Apr	2020	166	17.0	96	13.0
9 May	0712	205	18.0	103	14.0
21 May.....	2055	177	14.0	166	13.0
25 Jun	1550	184	16.0	136	15.1
29 Jun	0233	136	17.8	97	12.0
29 Jun	1041	198	17.0	138	13.5
29 Jun	1822	226	17.5	117	20.0
1 Jul	1626	168	25.0	93	17.0
21 Jul.....	0254	134	19.0	117	11.8
23 Aug	2127	192	15.0	167	12.5
24 Aug	1608	178	13.5	179	12.5
25 Aug	1256	140	14.0	87	11.7
24 Sep	0732	176	15.0	167	12.0
5 Nov	2226	168	15.0	168	16.5
5 Nov	2233	184	15.0	180	16.0
6 Nov	1725	136	12.5	76	11.0
19 Nov	0532	206	16.0	89	16.8

Nonthermal velocities derived from the spectral lines observed during flares with the FCS are relatively lower (Antonucci & Dodero 1995) because the FCS observations refer to later times of flare evolution (peak and decay). Nevertheless, both BCS and FCS results confirm that nonthermal velocities depend on plasma temperature.

4. DISCUSSION

In the following discussion, we assume that the plasma that originates the nonthermal line broadening is generated by a reconnecting current sheet—i.e., it is heated and accelerated within the current sheet and ejected from it—and we discuss the consistency of this hypothesis with the observational results and their implications.

The fact that the peak of nonthermal velocities, as observed in the Fe XXV–emitting plasma, is approximately coincident

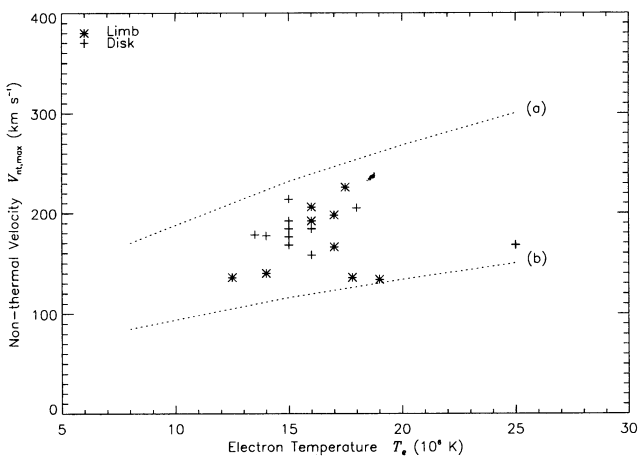

FIG. 2.—Highest value of nonthermal velocity $V_{nt,max}$ observed during a flare, as derived from the analysis of the Fe XXV spectra, plotted vs. plasma temperature. The results obtained from limb flares are indicated with asterisks and those from disk flares with crosses.

with flare onset and precedes by 30 s, on average, the peak of the hard X-ray emission points to a close relationship between nonthermal motion and the onset of energy release in flares. The precursory character of the enhanced nonthermal motion is even more evident when one studies enhanced Ca XIX nonthermal broadenings observed even earlier in the flare. This has led to the suggestion that the energy release and heating is initiated at a lower rate and then proceeds catastrophically (see, e.g., Antonucci et al. 1986, 1990). In consideration of the timing with respect to the hard X-ray emission, we can reasonably assume that the earlier line broadenings in Ca XIX are related to the preflare phase of reconnection in a current sheet and that the broadening of the Fe XXV lines is more probably related to the explosive and/or the "hot" phase of flares.

At the very beginning of a flare, the outflows from a current sheet are expected to be observed in the most favorable conditions. At this time, since the energy release is in its initial stage, the high-temperature plasma evaporating from the chromosphere is not yet predominant. As a consequence, for a limited period near flare onset we presume that the soft X-ray source observed in the flare region is mostly formed by high-temperature plasma produced by reconnecting current sheets and only in minor part from plasma evaporated from the chromosphere. This is in agreement with the fact that, early in the flare, evaporation can account only for ≤ 0.2–0.3 of the soft X-ray source (Antonucci et al. 1982).

Our analysis shows that the highest values of nonthermal velocities are indeed observed in the period preceding the major hard X-ray burst, that is, either when we observe a marginal input of chromospheric plasma into the corona or evaporation is still absent (50% of the cases). This ensures that the measured nonthermal peak velocities $V_{\rm nt,max}$ are in large degree associated with the material produced by the current sheet itself. Hence, the "turbulent" plasma at flare onset mainly carries information on the physical conditions within the current sheet itself.

The substantial longitude-independence of nonthermal velocities and the fact that peak velocities are in any case above 120 km s^{-1} (Fig. 2) may have different implications depending on the scale, geometry, and number of the current sheets. Let us consider the two limiting cases: a single, large-scale plane current sheet and numerous small-scale current sheets spread throughout the flare region. In the case of a single, large-scale current sheet oriented at a random angle β with respect to vertical (the random nature of β is implied by the longitude-independence of the observed nonthermal velocities), we expect, over a large number of flares and over flare longitude, a nonthermal velocity component along the LOS close to $\langle V_{\rm nt}\rangle = V_{\rm A}\langle\cos\beta\rangle\langle\cos\gamma\rangle$, γ being the angle between the vertical and the observer, which varies with flare longitude. Therefore, we obtain $V_{\rm nt} = \frac{1}{4}(1.2 \times 10^4)T_s^{1/2} = 3 \times 10^3 T_s^{1/2}$ cm s^{-1}.

In this hypothesis, though depending on the orientation of the current sheet, in individual events nonthermal velocities with values close to zero should also be observed, a case not verified by the set of events analyzed ($V_{\rm nt} \geq 120$ km s^{-1}). Hence, either the presence of a single, large-scale current sheet in the flare region is a rare event or the current-sheet geometry is in general more complex than assumed in the simple scheme of Figure 1. For example, the assumption of a curved current sheet implying a distribution of α angles could explain the observation $V_{\rm nt} \geq 120$ km s^{-1}. When the projection angle is almost uniformly distributed, for instance for a particularly complex configuration, the mean square value can be close to $\langle\cos\alpha\rangle \sim \frac{1}{2}$, the factor expected in the case of many small-scale current sheets, reconnecting in the flare region, oriented at random with respect to the LOS (§ 2.1). The emergence of plasma from a curved current sheet is potentially also a source of some degree of asymmetry in the velocity distribution and, therefore, in the spectral line profile.

Therefore, in the "hot" phase of flares both a large-scale, curved current sheet with a certain degree of complexity and many small-scale sheets can give an average nonthermal velocity along the line of sight $V_{\rm nt} = V(T_s) = 6 \times 10^3\ T_s^{1/2}$ cm s^{-1} (eq. [7] with $\langle\cos\alpha\rangle \sim \frac{1}{2}$). In the case of the rupture of the current sheet during the explosive phase, this value represents a lower limit on the velocity. The values of $V_{\rm nt}$ for plane current sheets would instead cluster around a curve $V \sim 3 \times 10^3\ T_s^{1/2}$ cm s^{-1}, but only when many flares were considered. According to Figure 2, the peak velocities $V_{\rm nt,max}$ observed near flare onset, when the hot plasma is presumably predominantly produced by the reconnecting current sheet, are limited by the two curves $V(T_s)$ predicted for $\langle\cos\alpha\rangle = \frac{1}{2}$ (*curve* "*a*") and $\langle\cos\alpha\rangle = \frac{1}{4}$ (*curve* "*b*").

The model velocities represented by the curves in Figure 2 pertain to a plasma that maintains approximately the same physical conditions attained inside the current sheet. However, once expelled into the region surrounding the current sheet, the plasma may undergo deceleration and cooling processes, primarily as a consequence of the temperature gradient established along the magnetic field lines connecting the current sheet with the ambient plasma. Therefore, even if we limit the discussion to flare onset, when evaporation is negligible, we expect to find the observational points at lower temperature and velocity than those predicted from the HTTCS model at the plasma's emergence from the current sheet. As a consequence, when allowing for cooling and deceleration, the experimental points can only be consistent with the upper curve (*a*) derived for $\langle\cos\alpha\rangle = \frac{1}{2}$. That is, the experimental results appear to be consistent with reconnection that occurs in many small reconnecting sheets within a flare region or, alternatively, within a large-scale current sheet with a complex configuration.

If we consider that the outflows undergo some deceleration and cooling before being observed, we can relate the observed nonthermal velocity $V_{\rm nt}$ to the temperature inside the reconnecting current sheet. In the simplifying approximations that a constant pressure is established after a limited initial time along the temperature gradient, $p = nkT = \text{const}$ (see discussion in Shmeleva & Syrovatskii 1973) and that the flow is confined in a magnetic flux tube with an average constant cross section $nV = \text{const}$, we find that the ratio between velocity and temperature remains constant:

$$\frac{V}{T} = \left(\frac{V}{T}\right)_s = \frac{V_{\rm A}(T_s)}{T_s}\,, \tag{19}$$

where $(V/T)_s$ is the value at the emergence from the reconnecting current sheet. By using equation (4), we can relate the velocity-temperature ratio T/V of outflows to the temperature T_s inside the reconnecting current sheet:

$$T_s = \left(\frac{T}{V}\right)^2 (1.2 \times 10^4)^2\ \text{K}\,. \tag{20}$$

If we take T/V to be the observed ratio $T_e/2V_{\rm nt}$, given that $V_{\rm nt} = V\langle\cos\alpha\rangle = V/2$, the experimental values ($V_{\rm nt}$, T_e) relative to the plasma that is undergoing cooling and deceleration

outside the current sheet can be directly related to the temperature of the plasma inside the current sheet by

$$T_s = 3.6 \times 10^7 \left(\frac{T_e}{V_{nt}}\right)^2 \text{ K} . \quad (21)$$

The experimental ratios T_e/V_{nt} fall within 0.7 and 1.5; therefore, the inferred temperature inside the reconnecting current sheet, T_s, is expected to be within (20–80) $\times 10^6$ K. As a consequence, the corresponding velocities $V_A(T_s)$ at the emergence of the reconnecting current sheet are within 500–1100 km s^{-1}.

5. CONCLUSIONS

Under the hypothesis that solar-flare energy release is associated with magnetic reconnection in a current sheet, we expect, at flare onset, plasma outflows with equal and opposite velocity components along the LOS, which result in a symmetric, nonthermal broadening of soft X-ray spectral lines, i.e., in the presence of nonthermal, "turbulent" veocities in the flare plasma. We interpret, therefore, the enhanced nonthermal motion observed in flare plasmas when the energy is initially released in terms of outflows from a reconnecting current sheet. At this time, the observed soft X-ray source consists mainly of plasma heated in the current sheet and expelled from it at the Alfvén velocity, and it carries direct information on the reconnecting region. According to the HTTCS model, the predicted nonthermal velocities depend on $T_s^{1/2}$, that is, they are a function of the temperature T_s inside the current sheet.

The observed nonthermal velocities, which attain their peak value at flare onset, just before the peak of the hard X-ray emission, i.e., before the energy release is at its maximum, have as an upper limit the curve $V(T_s) = 6 \times 10^3 T_s^{1/2}$ obtained from the HTTCS model for the "hot" phase of flare under the assumption that the projection angle of the current sheet with respect to the LOS is given by $\langle \cos \alpha \rangle = \frac{1}{2}$. The value $\langle \cos \alpha \rangle = \frac{1}{2}$ is obtained with the supposition that magnetic reconnection occurs either in many small-scale reconnecting current sheets with random orientation with respect to the LOS or in a curved, large-scale current sheet with an appropriate distribution of projection angles for the outflows. The fact that the data points are found to be below the model curve $V(T_s)$ can be explained by invoking cooling and deceleration processes of the outflows in the region surrounding the current sheet, which imply a decrease in the temperature-velocity values observed in the soft X-ray source relative to the conditions at the current sheet. Therefore, the observations can be considered to be consistent with the presence of macroscopic motions with equal and opposite velocity components along the LOS that are associated with the outflows expected either from many small-scale reconnecting current sheets or one, or few, large-scale, curved current sheets.

When considering the cooling and deceleration processes in the approximations of a constant–cross-section flux tube and constant pressure, the observed nonthermal velocity and temperature of the plasma in the flare region can be directly related to the temperature inside the reconnecting current sheet. The observations appear to be consistent with current sheets at temperatures $\lesssim 80 \times 10^6$ K and with initial outflow velocities at emergence from the current sheet $\lesssim 1100$ km s^{-1}.

We conclude that the predictions of the velocity of the outflows as a function of the temperature inside the current sheet based on the HTTCS model are substantially consistent with the spectral line observations, provided the soft X-ray source observed at flare onset consists mainly of plasma ejected from several small-scale or one/few curved, large-scale reconnecting current sheets. The number and/or geometrical complexity of the reconnecting current sheets ensures the substantial isotropy of the velocities in the flare region in such a way that the nonthermal velocity observed during flares becomes independent of flare longitude.

The authors wish to acknowledge the support of the Agenzia Spaziale Italiana and of the Ministero dell' Università e della Ricerca Scientifica e Tecnologica.

REFERENCES

Antonucci, E. 1986, Highlights Astron., 7, 731
———. 1989, Sol. Phys., 121, 31
Antonucci, E., et al. 1982, Sol. Phys., 78, 107
Antonucci, E., & Dodero, M. A. 1995, ApJ, 438, 480
Antonucci, E., Dodero, M. A., & Martin, R. 1990, ApJS, 73, 147
Antonucci, E., Gabriel, A. H., & Dennis, B. R. 1984, ApJ, 287, 917
Antonucci, E., Rosner, R., & Tsinganos, K. 1986, ApJ, 301, 975
Antonucci, E., & Somov, B. V. 1992 Coronal Streamers, Coronal Loops, and Coronal and Solar Wind Composition (ESA SP-348) (Noordwijk: ESA), 293
Doschek, G. A. 1989, ApJS, 73, 117
———. 1986, in Energetic Phenomena on the Sun, ed. M. Kundu & B. Woodgate (NASA CP-2439) (Greenbelt: NASA), 4-1
Doschek, G. A., et al. 1994, ApJ, 431, 888
Mariska, J. T. 1994, ApJ, 434, 756
Parker, E. N. 1957, J. Geophys. Res., 62, 509
Parker, E. N. 1979, Cosmic Magnetic Fields (Oxford: Clarendon)
Priest, E. R. 1982, Solar Magnetohydrodynamics (Dordrecht: Reidel)
Shmeleva, O. P., & Syrovatskii, S. I. 1973, Sol. Phys., 33, 341
Somov, B. V. 1992, Physical Processes in Solar Flares (Dordrecht: Kluwer)
———. 1994, Fundamentals of Cosmic Electrodynamics (Dordrecht: Kluwer)
Somov, B. V., & Syrovatskii, S. I. 1976, Proc. P. N. Lebedev Phys. Inst., 74, 13
Sweet, P. A. 1958, in IAU Symp. 6, Electromagnetic Phenomena in Cosmical Physics, ed. B. Lehnert (Cambridge: Cambridge Univ. Press), 123
Syrovatskii, S. I. 1976, Proc. P. N. Lebedev Phys. Inst., 74, 13
Syrovatskii, S. I., & Somov, B. V. 1980, in Solar and Interplanetary Dynamics, ed. M. Dryer & E. Tandberg-Hanssen (Dordrecht: Reidel), 425
Tandberg-Hanssen, E., & Emslie, A. G. 1988, The Physics of Solar Flares (Cambridge: Cambridge Univ. Press)
Zirin, H. 1987, Astrophysics of the Sun (Cambridge: Cambridge Univ. Press)